Ultrasonics Sonochemistry 71 (2021) 105360

Contents lists available at ScienceDirect

Ultrasonics Sonochemistry

journal homepage: www.elsevier.com/locate/ultson

The effect of sonication on the ion exchange constant, K_X^{Br} of CTABr/chlorobenzoates micellar systems

Nor Saadah Mohd Yusof

Department of Chemistry, Faculty of Science, University of Malaya, 50603 Kuala Lumpur, Malaysia

ARTICLE INFO

Keywords:
Ultrasound
Micelle
Ion exchange
Viscoelasticity
Micelle growth

ABSTRACT

The ion exchange constant, K_X^{Br} (for the case of cetyltrimethylammonium bromide, CTABr, in this study) is a method dependant characterization of ion exchange process by counterions, X and Br with different relative binding ratios. In this report, the ion exchange constant, K_X^{Br} values for micelle systems irradiated under 2 min of sonication at 120 W power using a probe sonicator with 1 cm tip were determined to be 85.2, 125.6 and 122.4 when X = *o*-, *m*- and *p*-chlorobenzoates, respectively. The values were quantified using a semiempirical kinetic method coupled with Pseudophase Micellar model, and later compared to the same system in the absence of sonication. The sonication was found to amplify the K_X^{Br} values by ~ 13-fold for X = *o*-chlorobenzoate and ~ 2.5-fold for X = *m*- and *p*-chlorobenzoates. This is due to the improvement of ion exchange process by the oscillation of bubbles generated by acoustic cavitation. An active ion exchange process indicates better stabilization of the micelle aggregational structure by the penetration of the introduced counterions, X into the micelle Stern layer leading to the growth of the micelle. This is supported by the remarkable increase in the viscosity of the micelle system by > 7-fold for X = *o*-chlorobenzoate and by > 2-folds for X = *m*- and *p*-chlorobenzoates. Sonication was also found to induce maximum viscoelasticity at lower concentration ratio of [CTABr]:[X]. The ability of ultrasound to induce micelle growth and exhibiting viscoelasticity at lower concentration of counterionic additive will be very useful in technologies where viscoelastic solution is desired such as in oil drilling and centralized heating and cooling system.

1. Introduction

Micelles are known to play prominent roles in many processes in both fundamental and applied science. The dissolution of micelle monomers above its critical micelle concentration and Kraft temperature will result in aggregations as a mean to achieve their thermodynamic stability when exposed to solvents [1–5]. Their ability to protect the hydrophobic tails in aqueous medium allows remarkable solubilizing properties of hydrophobic molecules [6,7]. This is especially useful for the development of daily home products and during the design of drug delivery carriers. A similar behaviour is also seen when they form inverse micelle aggregations in nonpolar solvents. Apart from that, aqueous solutions of micelle systems exhibiting viscoelasticity have also been actively studied due to their remarkable rheological properties and large variety of applications. Naming a few are as household products [8,9], petrochemicals [10,11], pharmaceuticals [7], in heating and cooling systems [12,13], and health and drug delivery systems [7,14]. The interest to utilize micelles in new products and technologies are mainly due to two of its controllable properties: (i) their amphiphilicity and flexibility to form normal or inverse micelle structures, and (ii) their reversible aggregational responses upon stimuli manipulation.

Though micelles are known to form spherical structures, they can aggregate to form various structures as their attempt to minimize their free energies [1,2]. As they grow, the water like solution gradually becomes more viscous. When the aggregation forms elongated flexible structures termed as “wormlike” or “threadlike” micelle, the viscoelasticity of the system will be visible. Such aggregations occur when the small micellar aggregates grow in one direction and form very long and flexible network. This only occurs above a defined concentration and conditions in which they entangled into a dynamic network and overlapping with each other. This results in a remarkable viscoelasticity, similar to solutions of flexible polymers [15,16]. However, unlike the rigidity exhibited by polymers in solution, wormlike micelles possess a special ability to break and reform under the manipulation of stimuli, thus usually referred to as “living polymers” [17].

The micelle aggregational growth/de-growth relies on the

E-mail address: adah@um.edu.my.

https://doi.org/10.1016/j.ultsonch.2020.105360
Received 21 September 2020; Received in revised form 4 October 2020; Accepted 5 October 2020
Available online 15 October 2020

competitive thermodynamic balance between the attractive force of their hydrophobic tails that favour the aggregation of micelle monomers, as well as the repulsive force of their charged heads that limit its aggregation size [18]. The initial study in this area reported that such induced aggregational growth may be stimulated by the introduction of suitable additives. Naming a few of the extensively studied polymeric micelles interaction with various additives are the cationic cetyltrimethylammonium bromide, the anionic sodium dodecyl sulphate and Pluronic micelles. The additives added can either be the oppositely charged cosurfactants [19,20], hydrophobic counterions [21] or specific targeting ligand molecules [22]. The introduction of the additives results in the dehydration of micelle core as well as the reduction of micelle heads repulsion, thus increasing their stability and promoting growth [23]. Despite the excellent micelle structural responses towards the introduction of additives, certain application requires properties exhibited by grown micelles without the addition of too much additives. This is especially important in technologies such as drug delivery systems where such additives might cause certain side effects to the body, and in oil drilling technology where such additives might be harmful to the environment. Therefore, recently there are many attempts to manipulate micelle aggregational structure by various types of stimuli. Some examples are by changing the solution pH [24,25] or temperature [26–28], exposing the solution to UV light [28], and others. Recently, it was reported that ultrasound is able to induce changes in micelle structures [5]. In certain conditions, ultrasound was reported to break micelle structures, changing a viscoelastic system to water like solution [29]. Under different sonication condition, the viscoelasticity may be induced, and even enhanced in the presence of minimal amount of suitable counterions [5,30].

In this study, the ion exchange constant (K_X^{Br}) values for cetyltrimethylammonium bromide (CTABr) micelle system in the presence of various chlorobenzoic acids (X), where X = *o*-, *m*- or *p*-chlorobenzoic acids under the influence of sonication were calculated and compared to the previous study of the same system without sonication [21]. The ion exchange constant values are indicative of the micelle structural transformation degrees from spherical to rodlike to wormlike to threadlike/polymeric micelles. The lengthening of the micelle aggregation may be directly observed by the increasing viscoelasticity behaviour of the solution as well as the achievement of such viscoelasticity in the presence of minimal volume of X. This study predicts that a) ultrasound promotes structural transformations of the cationic CTABr micelle system in the presence of various chlorobenzoic acids, X, and b) ultrasound-induced transformation is in the order of *o*-chlorobenzoic acid > *m*-chlorobenzoic acid ≈ *p*-chlorobenzoic acid. In other words, the micelle growth can be intelligently manipulated by the combination of ultrasound action and the choice of additive, even when the amount of additive present is minimal. Inducing viscoelasticity without excessive introduction of the additives is significant when a superviscoelastic micelle system is required such as in the centralized heating and cooling solution or in enhanced oil recovery solution, and when minimal amount of carrier material is aimed for applications such as drug delivery.

2. Materials and methods

2.1. Materials and equipment

The chemicals used for the experiments were reagent grade phenyl salicylic acid (≥98% from Fluka), cetyltrimethylammonium bromide (CTABr) (≥99% from Fluka), piperidine (≥99% from Merck), and *o*-, *m*- and *p*-chlorobenzoic acids (≥98% from Merck). All of them were commercial products of the highest available purity, thus used as received. However, *o*-, *m*- and *p*-chlorobenzoic acids were recrystallized before use to avoid unnecessary background absorbance during UV measurements. The kinetics experiments were carried out in aqueous system, but the stock solution of 0.01 M phenyl salicylate was prepared in acetonitrile due to its limited solubility in water. The stock solutions of 0.5 M of *o*-, *m*- and *p*-chlorobenzoates were prepared by adding 0.55 M sodium hydroxide. This was to replace the acidic hydrogens on the acids. The solution composition was kept the same for kinetics and rheological measurement.

During kinetics experiments, phenyl salicylate was monitored using Shimadzu UV–visible 1650 absorption spectrophotometer equipped with electronically controlled thermostatic cell compartment set at 35 °C. The rheological measurements were carried out using Anton Paar MCR301 rheometer, using a double gap cylinder, DG26.7/T200/SS with 24.656 mm internal diameter and 26.661 mm external diameter. The temperature was controlled at 35 °C using the Peltier temperature control unit.

2.2. Ion exchange constant determination

The rate of the nucleophilic reaction of piperidine with phenyl salicylate was measured spectrophotometrically at 35 °C by monitoring the disappearance of the reactant, phenyl salicylate, at 350 nm as a function of reaction time. The experimental solution was prepared by adding 2×10^{-4} M phenyl salicylate, 0.1 M piperidine, > 0.03 M NaOH, 5 mM CTABr and concentrations of *o*-, *m*- or *p*-chlorobenzoic acids ranging from 0 to 0.1 M. Deionized water was added to make up a total sample volume of 5 mL. The reaction between piperidine and phenyl salicylate was reported to result in the formation of *N*-piperidinylsalicylamide and phenol via an intramolecular general base assistance reaction, in aqueous system. The details of the product characterization was described elsewhere [31]. The solution was then sonicated at 20 kHz (Branson), 120 W power using a probe sonicator with 1 cm tip horn for 2 min. The sonication duration was fixed to allow ultrasound-induced ion exchange process, but without any undesired individual effect on the chemicals present in the sample solution. The characteristic apparent molar absorptivity of the reaction was unchanged even under the influence of sonication, indicating that the reaction and the product from the piperidinolysis of phenyl salicylate was unchanged. Nonlinear least-squares technique was used to calculate the kinetic parameters which included the pseudo first order rate constant, k_{obs}; apparent molar absorptivity of the reaction mixture, δ_{app} and the final absorption, A_∞. The pseudo first order equation is given in Equation (1) below

$$A_{obs} = [PS_0]\delta_{app}\exp(-k_{obs}t) + A_\infty \quad (1)$$

In Equation (1), A_{obs} is the absorbance shown by the reaction mixture over reaction time, $[PS_0]$ is the initial concentration of phenyl salicylate ($[PS_0] = 2 \times 10^{-4}$ M) and t is the reaction time. All the kinetic runs were carried out until the absorbance reaches plateau.

2.3. Rheological measurements

The sample composition for rheological measurement was the same as for kinetics measurements, with total volume of 25 mL. Steady shear and dynamic shear rheological measurements were carried out within the shear rate (γ) range and oscillatory frequency (ω) range of 0.01 to 1000 s^{-1} and 0.1 to 100 $rads^{-1}$, respectively. This was within the linear viscoelastic regime where the storage (G') and loss (G'') moduli remain independent of the strain amplitude.

3. Results and discussion

3.1. The ion exchange values (K_X^{Br}) of cationic CTABr/chlorobenzoates micelle systems

As micelle monomers such as CTABr aggregate together, the positively charged hydrophilic heads of CTA^+ point out of the micelle

aggregation towards the aqueous bulk phase, as described by the Stigter model [4]. This structural aggregation is encouraged by the hydrophobic attraction of their tails, to be away from water when dissolved in aqueous solutions. On the other hand, the same charge heads repel from each other, therefore, need to be stabilized by their counterions, Br^-. This is achieved by the distribution of the intercalated Br^- ions between the positively charged micelle heads. When another counterion, X^- is added into the system, X^- enters the micellar pseudophase and pushes Br^- out to certain extent [32]. The factors governing the ability of one counterion pushing out the other depends on the binding degree of each of those counterions to the micelle. Therefore, the nature of the counterions such as its hydrophobicity, the hydrated size, valence are lipophilicity need to be considered when predicting and developing such micelle solution [32]. In the system reported in this study, X^- is a larger, more hydrophobic counterion than Br^-, and is able to penetrate deeper and bound better into the CTA^+ micelle pseudophase. These relative binding ratios where X^- and Br^- are the competing counterions in the cationic micellar system is represented by the ion exchange constant, K_X^{Br}, or also known as the ion selectivity constant.

The occurrence of ion exchange between counterions present was initially reported towards the end of 1960s [33,34]. It was amongst the first factor to be known to be able to promote and manipulate the reversibility and flexibility of micelle aggregation. Over the following years, there had been numerous attempts to quantify the ion exchange constants using various chemical and physical techniques [35–38]. An example is a system involving CTABr and sodium hydroxynaphthalene where the change from vesicle to wormlike micelle upon heating from room temperature to 70°C was reported [39]. This is due to the effect of temperature on the solubility of sodium hydroxynaphthalene, thus increasing the ion exchange efficiency. There had been numerous similar reports on specific responses of the counter-additives upon various stimuli such as pH and UV, thus increasing/decreasing the ion exchange process, and initiating micelle aggregation transformations [40,41]. Unfortunately, the ion exchange constant values were found to show significant deviation from study to study [37,42]. An example is the addition of 2,6-dichlorobenzoate on cetyltrimethylammonium chloride micelle system which resulted in the ion exchange constant values to be 16.2 ± 5.5 when measured using ^{1}H NMR measurement method and 1.3 ± 0.1 when measured using ion selective electrode measurement method [37,42]. Such glaring difference make it hard for the values to be referred to and compared with when the ion exchange and micelle growth process are being discussed. The method dependant values were contributed by the experimental deviation of the micelle system which is sensitive to its environment. Some variations that could significantly affect the ion exchange constant quantification are the extent of water concentration [43], the solubilizates' dispersion by their specific structure and hydrophobicity [44,45], ionic strength [46], and polarity [47] of the micelle in aqueous system. Therefore, in order for us to focus on the effect of ultrasound on CTABr/chlorobenzoates systems, this study utilizes one well established semi empirical kinetic method during the determination of ion exchange constants [21,42,48]. This method had successfully been used to quantify consistent values of ion exchange constants for systems involving various micelle and counterions, thus allowing reliable quantification and comparison within broader system. Using the same technique, this study aims to understand the *effect of ultrasound* on the CTABr aggregation structure in the presence of *o*-, *m*- and *p*-chlorobenzoates counterions. The details of the semi empirical kinetics method will be elaborated in the following section.

3.2. Determination of the ion exchange Constant, K_X^{Br}

The early studies of kinetics method in quantifying ion exchange constant involved the use of Pseudophase Ion Exchange (PIE) and mass action models [35,36]. However, reports have shown that the use of Pseudophase Micellar (PM) model serves a better purpose at kinetic quantification of the ion exchange process [49,50]. For instance, when the kinetic probe moves from the bulk aqueous to the micellar pseudophase, the PIE model only describes its activation based on the free energies of the reactants and ionic transition state. Whilst, PM model is able to consider the free energies of movement from the aqueous into the aggregation [49,51]. In addition to that, PIE showed an excellent fit only for system involving inert surfactant, whilst PM model is also applicable for spontaneous and reactive ion surfactant, as well as nonionic reactants [36,49]. Taking those into consideration, the semiempirical kinetics method used in this study to quantify the ion exchange process in an aqueous micelle system combines the concept of PM model with an empirical Equation (2) below.

$$K_S = \frac{K_S^0}{1 + K_{X/S}[X]} \tag{2}$$

In the above equation, X and S are two examples of counterions present. $K_{X/S}$ is an empirical constant that measures the ability of X to push S out of the micellar pseudophase into the bulk aqueous solution. This happens by the action of ion exchange between X and S. K_S and K_S^0 are the micelle binding constants of counterion S with and without the influence of counterion X. X and S are anionic counterions (X^- and S^-) for cases involving the cationic micelle systems, such as CTABr (CTA^+) in this study. When more counterions are present, say Y, the ion exchange constant, K_X^Y between X^- and Y^- can be calculated by the ratio of the two, as shown in Equation (3) below.

$$K_X^Y = \frac{K_{X/S}}{K_{Y/S}} \tag{3}$$

In this report, where CTABr is being studied, the Y species is the counterion of CTA^+, which is Br^-. X^- is the various *o*-, *m*- and *p*-chlorobenzoates. $K_{Br/S}$was calculated previously using the same method and found to be 25 [48]. The detection of the medium where counterion S resides due to ion exchange process is elaborated below.

For Equation (3) to be applicable, the counterion S must exhibit detectable properties, with significant difference according to the media it resides in. In this study, S is the phenyl salicylate ion and can be monitored well using UV–visible spectrophotometer. With the addition of piperidine at 1:500 ratio, the pseudo first order piperidinolysis of phenyl salicylate reaction takes place. As can be seen in Table 2, the rate of reaction shows more than tenfold decrease of reaction rate in micelle pseudophase as to aqueous phase (from 34.5×10^{-3} s^{-1} to ~ 32.2×10^{-4} s^{-1}). Such significant change makes it easy to detect the change of reaction medium, thus the extent of ion exchange involving phenyl salicylate upon the introduction of X. In previous study, the rate of reaction in aqueous phase were found to be 32.7×10^{-3} s^{-1} in the absence of ultrasound [48]. But upon the introduction of 5 mM CTABr micelle, the rate of reaction was also found to decrease by more than tenfold [48]. The change of the media where the reaction is taking place is illustration in Fig. 1below.

However, when the counterion *o*-, *m*- and *p*-chlorobenzoate is added, the counterion pushes phenyl salicylate from micelle pseudophase to aqueous phase by ion exchange process. As more of the reaction taking place in aqueous phase, the rate of reaction increases as can be seen in Fig. 2 and Table 1 below.

The increase of rate of reaction (k_{obs}) upon increasing concentration of either *o*-, *m*- or *p*- chlorobenzoates as shown in Table 1 were calculated according to the empirical Equation 4, where k_0 is the k_{obs} when [X] = 0 and [CTABr] ≠ 0; and $F_{X/S}$ and θ are the empirical constants. θ is represented in Equation 5 where k_w^X is the k_{obs} in aqueous media ([CTABr] = 0). The calculated values are shown in Table 2 below. The optimum concentration of X ($[X]_0^{op}$) is taken by identifying the lowest error (Σdi^2) values for each calculation. This is probably due to the shift of cmc under the reaction condition in this study. The $F_{X/S}$, $K_{X/S}^n$ and ion exchange constant, K_X^{Br} are also summarized in the table.

quation 4

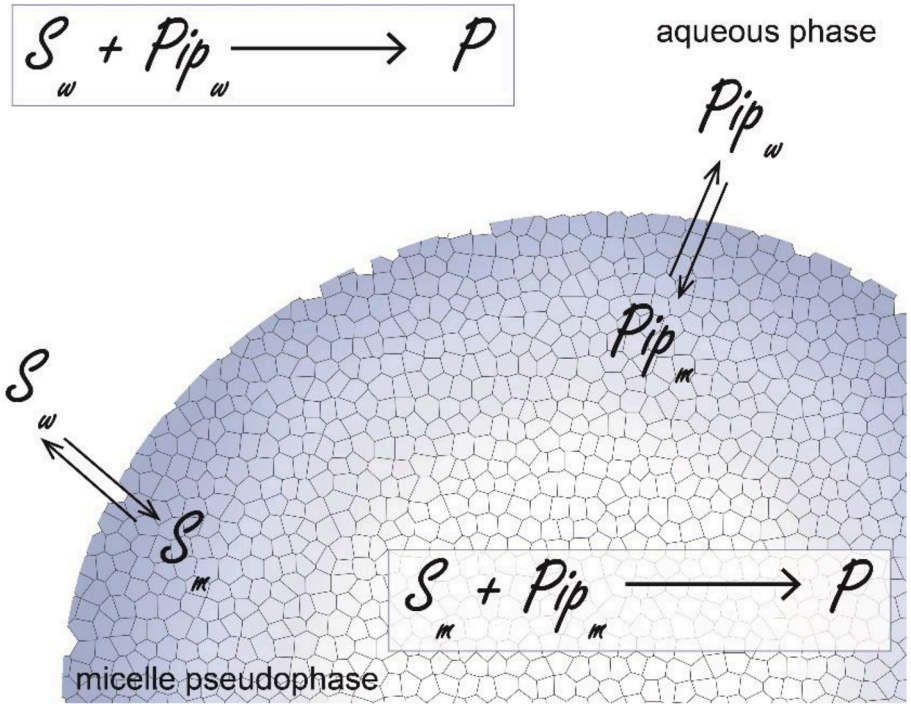

Fig. 1. The movement of both the reactants; phenyl salicylate between aqueous phase (S_w) and micelle pseudophase (S_m), $S_w \rightleftharpoons S_m$; and piperidine between aqueous phase (Pip_w) and micelle pseudophase (Pip_m), $Pip_w \rightleftharpoons Pip_m$. Phenyl salicylate and piperidine will react in both; aqueous phase ($S_w + Pip_w \rightarrow P$) and micelle pseudophase ($S_m + Pip_m \rightarrow P$) to form the same product with different rate of reaction.

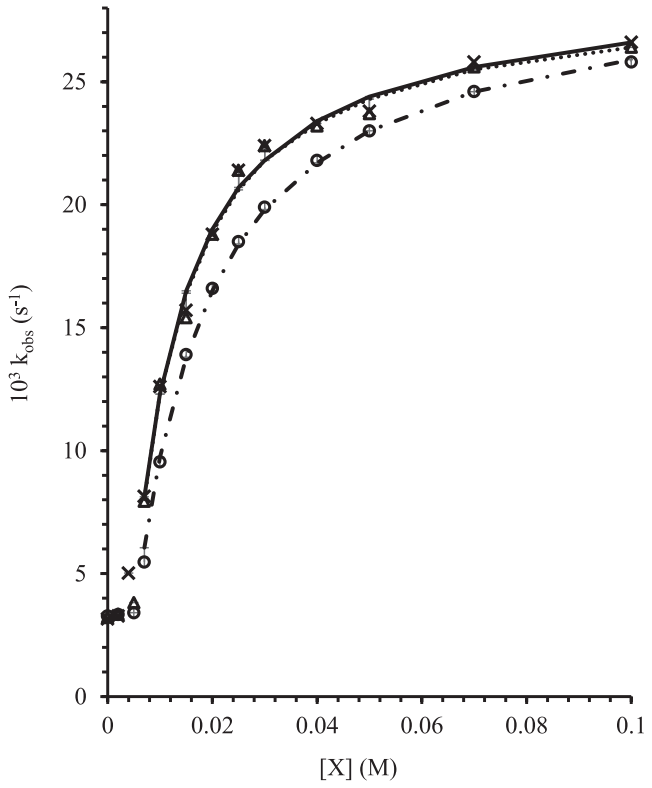

Fig. 2. The increasing k_{obs} upon increasing concentration of X, for the piperidinolysis of phenyl salicylate reaction at 35 °C. X are o-chlorobenzoate (○), m-chlorobenzoate (×) and p-chlorobenzoate(Δ). The lines are drawn through the calculated rate (k_{calc}) for o-chlorobenzoate (dashed), m-chlorobenzoate (solid) and p-chlorobenzoate (dotted) with kinetic parameters (k_0, θ and $K_{X/S}$) listed in Table 2 at$[MX]_0^{op}$ = 5.3, 4.7 and 4.8 mM, respectively.

$$k_{obs} = \frac{k_0 + F_{X/S}k_w^X K^{X/S}[X]}{1 + K^{X/S}[X]}$$

$$\theta = F_{X/S}k_w^X$$

As the counterion penetrates into the micelle Stern layer, promoting ion exchange, the micelle heads repulsion decreases, thus promoting growth. This became the basis for the prediction of the systematic correlation between ion exchange constant value with the efficient aggregation and growth. For instance, in the case of CTABr micelle in this study, if the micellar binding constant when counterion X is present (K_X^{Br}) is greater than the micellar binding constant when counterion Y is present (K_Y^{Br}), it is expected that the growth of the micelle in the system involving X is more than the system involving Y. We could also predict that the system when counterion X is present will show more viscoelasticity than when Y is present. The reliable quantification of ion exchange constants allows systematic prediction of the degree of micelle aggregational structure.

3.3. Ultrasonic responsive CTABr/chlorobenzoates micelle system as quantified by their ion exchange constant values

Though certain stimuli are able to promote structural changes of micelles [52–54], the utilization of ultrasonic energy is amongst the favoured as it could minimize the introduction of new material(s) to the micelle system, apart from being easily manipulated experimentally. Some examples of the various areas incorporating ultrasonication treatment of micelle in chemical processes are the degradation of contaminants in some industries such as electrical and electronics [52], for the synthesis of metal nanoparticles [55], during monomerization of photosentisizer used for cancer photodynamic therapy [53], and others. In drug delivery system, ultrasound can be used to trigger the drug release at specific time and space by disrupting the aggregation structure of micelle. This will increase the efficiency of the drug activity in specific region and timing, and reduces the side effect of the drugs to other healthy tissues. It is getting serious attention mainly because ultrasound

Table 1
The rate of reaction for the piperidinolysis of phenyl salicylate where [phenyl salicylate]$_0 = 2 \times 10^{-4}$ M, and [piperidine]$_T = 0.1$ M in aqueous system and 2% v/v CH_3CN. Residual error (RE) limits are standard deviations.

o-chlorobenzoate				*m*-chlorobenzoate				*p*-chlorobenzoate			
[X] (mM)	$10^3\,k_{obs}(s^{-1})$	$10^3\,k_{calc}(s^{-1})$	RE (%)	[MX] (mM)	$10^3\,k_{obs}(s^{-1})$	$10^3\,k_{calc}(s^{-1})$	RE (%)	[MX] (mM)	$10^3\,k_{obs}(s^{-1})$	$10^3\,k_{calc}(s^{-1})$	RE (%)
0	3.28			0	3.16			0	3.23		
2	3.34			2	3.28			2	3.35		
5	3.41			4	5.02			5	3.82	3.76	1.7
7	5.47	6.05	−11	7	8.14	8.13	0.1	7	7.94	8.03	−1.2
10	9.54	9.73	−1.9	10	12.6	12.3	2.2	10	12.7	12.3	3.5
15	13.9	13.8	0.6	15	15.7	16.5	−5.0	15	15.4	16.4	−6.8
20	16.6	16.5	0.7	20	18.8	19.0	−1.0	20	18.8	18.9	−0.7
25	18.5	18.4	0.6	25	21.4	20.7	3.5	25	21.4	20.6	3.8
30	19.9	19.8	0.6	30	22.4	21.8	2.5	30	22.4	21.8	2.9
40	21.8	21.7	0.3	40	23.3	23.4	−0.5	40	23.2	23.3	−0.5
50	23.0	23.0	−0.1	50	23.8	24.4	−2.7	50	23.7	24.3	−2.6
70	24.6	24.6	−0.1	70	25.8	25.6	0.6	70	25.6	25.5	0.4
100	25.8	25.9	−0.5	100	26.6	26.6	0	100	26.4	26.4	−0.1

Table 2
The empirical constant, θ and $K^{X/S}$ calculated from Equation 4 and Equation 5 for [CTABr]$_T = 5$ mM micelle system in the presence of various chlorobenzoates using nonzero.$[MX]_0^{op}$ values.

MX	$[MX]_0^{op}$(mM)	$10^4\,k_0(s^{-1})$	$10^4\,\theta(s^{-1})$	$F_{X/S}$[a]	$K^{X/S}(M^{-1})$	$K_{X/S}$[b](M^{-1})	$K^n_{X/S}$[c](M^{-1})	K^{Br}_X[d]
	Absence of ultrasound[e]							
2-chlorobenzoate	0	27.6	224 ± 6.9	0.69	6.56 ± 6.9	236.2	163	6.5
3-chlorobenzoate	6.0	30.7	266 ± 2.5	0.61	40.7 ± 1.4	1465	1192	47.7
4-chlorobenzoate	5.6	29.1	223 ± 4.1	0.68	49.6 ± 2.7	1786	1214	48.9
	Presence of ultrasound							
2-chlorobenzoate	5.3	32.8 ± 1.1[f]	293.5 ± 2.7[f]	0.85	69.6 ± 2.2[f]	2505	2129	85.2
3-chlorobenzoate	4.7	31.6 ± 0.9	290.0 ± 3.2	0.84	103.8 ± 6.8	3737	3139	125.6
4-chlorobenzoate	4.8	32.3 ± 1.0	287.4 ± 5.0	0.83	102.4 ± 7.0	3686	3059	122.4

[a] $F_{X/S} = \theta/k_w$ where $k_w = k_{obs}$ at $[CTABr]_T = 0$ at 35 °C, $k_w = 34.5x10^{-3}s^{-1}$.
[b] $K_{X/S} = K^{X/S}(1 + K^0_S[CTABr]_T)$ where $K^0_S = 7000M^{-1}$.
[c] $K^n_{X/S} = F_{X/S}K_{X/S}$.
[d] $K^{Br}_X = K^n_{X/S}/K^n_{Br/S}$ where $K^n_{Br/S} = 25M^{-1}$.
[e] Taken from [21].
[f] Error limits are standard deviations.

is non-invasive, therefore no insertion or surgery is required. However, the influence of ultrasound on micelle aggregation structures vary according to the sonication parameters and the micelle system being studied. Some studies reported degrowth of micelle aggregation, visible by the viscous to water like properties exhibited. An example is the sonication of sodium dodecyl sulphate (SDS) micelle system which resulted in the decrease of its spherical micelle diameter from 6 to 4.6 nm [54]. In another study, a system of dodecyl benzene sulfonate was found to be degraded when sonicated at 20 kHz frequency and 250 W of power for 250 min [52]. On the other hand, there were also studies that reports on the ability of ultrasound in inducing micelle growth [5,30].

As can be seen from Table 2, sonicating the micelle system in this study for 2 min at 20 kHz and 120 W power promoted the ion exchange process, thus resulting in consistent significant increase of K^{Br}_X values. The comparison of K^{Br}_X values for *o*-, *m*- and *p*-chlorobenzoates in the presence and absence of sonication are also represented in Fig. 3 above, where sonication increases the K^{Br}_X by ~ 13-folds for system involving *o*-chlorobenzoate, and ~ 2.5-folds for systems involving *m*- and *p*- chlorobenzoates. The main reason for this increment is due to the increasing binding of X on the micelle aggregational structure. This can be seen by the increase of the $F_{X/S}$ values from ~ 0.66 to ~ 0.84 as listed in Table 2. Stronger binding of X^- to CTA^+ micelle system forces phenyl salicylate ion from micellar pseudophase out to aqueous phase, thus increasing the reaction rate. Better binding of X^- stabilizes the repulsion between CTA^+ micelle heads, thus promoting micelle growth.

In the absence of ultrasonication, the ion exchange constant for system composed of CTABr/*o*-chlorobenzoate was 6.5 [21]. This

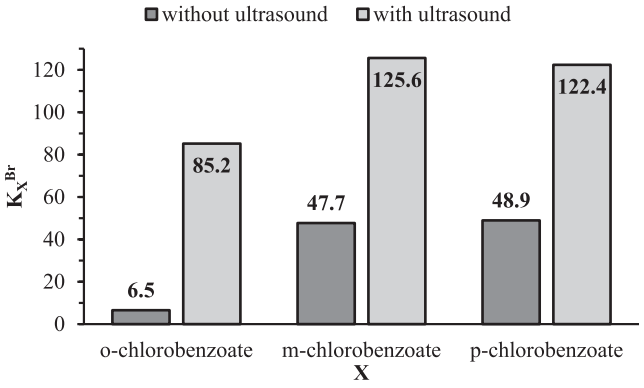

Fig. 3. The ion exchange constant, K^{Br}_X values for CTABr/o-, m- and p-chlorobenzoates in the presence and absence of sonication [21].

indicates weak ion exchange process when *o*-chlorobenzoate was added to the system. However, under the influence of ultrasonication, the K^{Br}_X value is significantly increased to 85.2, indicating more active ion exchange process upon the introduction of *o*-chlorobenzoate under the influence of sonication, thus micelle lengthening. This is supported by the rheological data in Fig. 4 below. The maximum viscosity for system involving *o*-chlorobenzoate was found to increase by >7-folds (0.76 to 5.97 Pa.s) when sonicated. Similar trend were also seen for system involving CTABr/X where X is *m*- or *p*-chlorobenzoates. The K^{Br}_X values

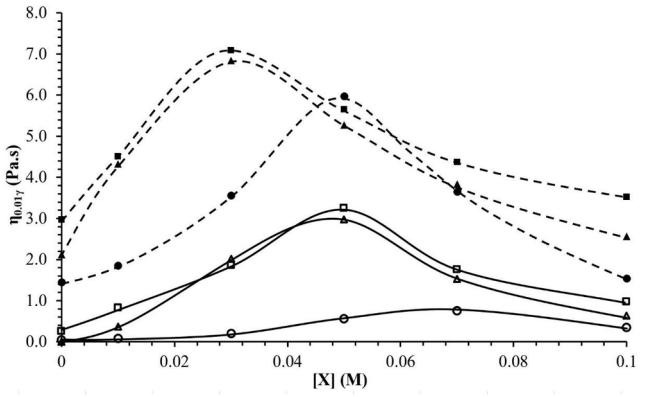

Fig. 4. The viscosity ($\eta_{0.01\gamma}$) of CTABr/X micelle solutions where X is o-chlorobenzoate (○,●), m-chlorobenzoate (Δ,▲) and p-chlorobenzoate (□,■). The solid lines are plotted for micelle systems without sonication, and the dashed lines are plotted for micelle systems under sonication.

reported without sonication were 47.7 and 48.9, for when X = *m*- and *p*-chlorobenzoates, respectively [21]. Based on the K_X^{Br} values, limited lengthening of micelle aggregation were predicted. Again, when the systems were sonicated, the K_X^{Br} values increase to 125.6 and 122.4 for when X = *m*- and *p*-chlorobenzoates, respectively. Such increment indicates glaringly improved ion exchange process, thus significant micelle lengthening. These are supported by the viscosities increase by >2-fold (2.98 to 6.84 Pa.s for *m*-chlorobenzoate, and 3.25 to 7.09 Pa.s for *p*-chlorobenzoate) shown in Fig. 4 below. Apart from that, it is also important to note that sonication is able to induce maximum viscoelasticity at lower amount of counterion required. Shown in Fig. 4 that the [CTABr]:[X] volume composition where the maximum viscosities were observed shifted from 5:70 mM to 5:50 mM for when X = *o*-chlorobenzoate, and from 5:50 mM to 5:30 mM for when X = *m*- and *p*-chlorobenzoates. This clearly suggests that not only sonication increases the binding, thus the ion exchange constant; but sonication also improves the efficiency of counterion in inducing viscoelasticity (Fig. 5). This will significantly improve the preparation design of surfactant solutions in applications where viscoelasticity is required such as the viscoelastic surfactant in oil drilling and in cooling and heating system .

Looking closely at the effect of sonication on CTABr/chlorobenzoates micelle systems, the increment of the K_X^{Br} and viscosity values are more prominent in system involving *o*-chlorobenzoate as compared with the systems involving *m*- and *p*-chlorobenzoates. This is due to the less viscous system formed when X = *o*-chlorobenzoate. In other words, the ability of ultrasound to induce micelle growth decreases when viscosity of the solution increases. The less viscous solution allows better oscillation of the nanobubbles, thus inducing more ion exchange process. On the other hand, the more viscous solution results in greater attenuation of ultrasonic waves, thus resulting in less effect on the ion exchange process. This indicates that the increased ion exchange process is mainly due to the oscillating microbubbles generated by acoustic cavitation. This ion exchange processes in the presence and absence of ultrasounication are illustrated in Fig. 4 (a) and (b) below, respectively.

The acoustic cavitation generates microbubbles which oscillate to their maximum resonance size and implode [56]. In micelle pseudophase system, significantly smaller bubbles also known as nanobubbles are formed either by acoustic cavitation or by cavitation formed by air-hydrophobic interface [57]. These bubbles oscillate, and due to the viscosity of the micelle solution, the nanobubbles oscillate longer [57] and implode with less intensity, as shown in the magnified inset of Fig. 4 (a). The action of the nanobubbles allows more of the counterion X to penetrate into the micelle Stern layer ($X_w \rightarrow X_m$). This pushes more of the phenylsalicylate out ($S_m \rightarrow S_w$), by the process of ion exchange. As the more hydrophobic counterion penetrates deeper, the CTA^+ heads repulsion is reduced, allowing the growth of micelle structure. This can

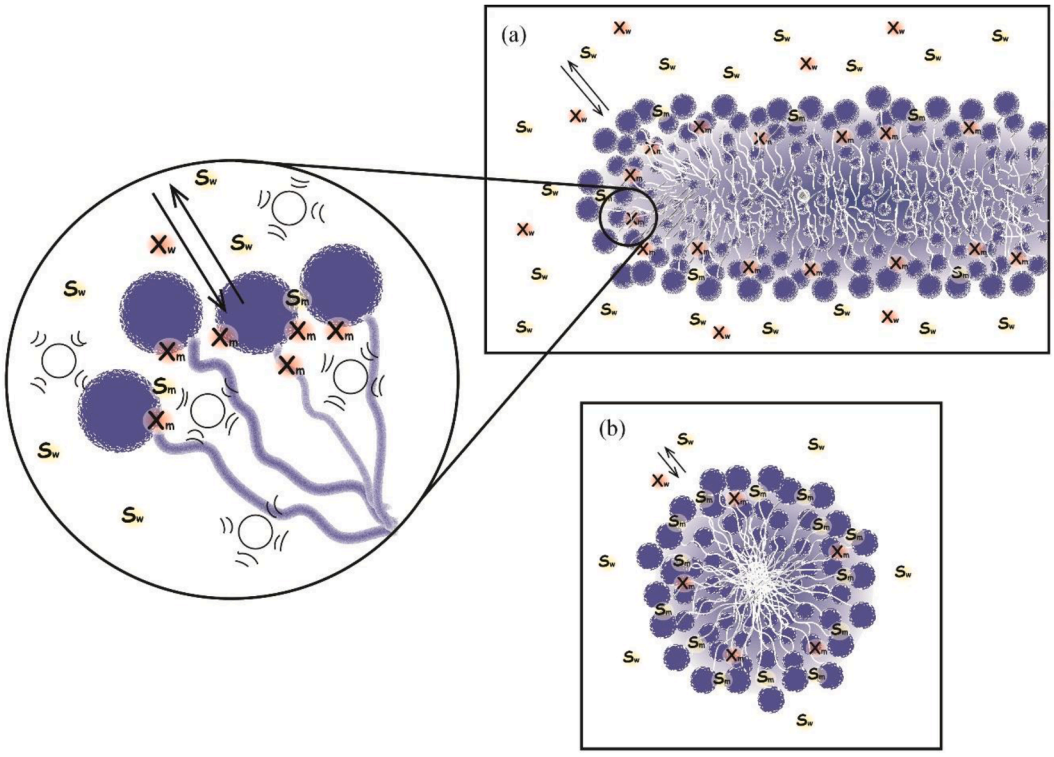

Fig. 5. (a) The ion exchange process in the presence of ultrasonication. The oscillating microbubbles (○) as shown in inset induce better penetration of counterion X from aquoeus phase (X_w) to micellar pseudophase (X_m). This pushes more S from micelle pseudophase (S_m) to aqueous phase (S_w). (b) The ion exchange process in the absence of ultrasonication. Without the amplified ion exchange process by the action of oscillating microbubbles, less X penetrates from aqueous phase (X_w) to micelle pseudophase (X_m), thus limited micelle growth.

be seen by the many phenyl salicylate in aqueous phase ($S_w > S_m$) and also evident by the increasing rate of reaction observed. The effect of sonication can be compared to the many phenyl salicylate in micelle pseudophase ($S_m > S_w$) as illustrated in Fig. 4 (b). In this case, the penetration of X into micelle Stern layer is not aided by the micro-bubbles oscillation, thus limited as quantified by their ion exchange constant values.

4. Conclusion

The work reported in this study demonstrates the ability of ultrasound to induce micelle aggregational growth, thus greater viscoelasticity with CTABr/chlorobenzoates micelle systems. The maximum viscoelasticity was also achieved at lower concentration of chlorobenzoates required. The extent of micelle growth was quantified by the ion exchange constant, K_X^{Br} values determined by the semiempirical kinetic method coupled with Pseudophase Micellar model. The viscoelasticity was studied using rheological measurements. The oscillation of the bubbles generated by acoustic cavitation improves the penetration and binding of the chlorobenzoates, thus ion exchange process. This action by ultrasound induces micelle growth. It can be anticipated that the ability of ultrasound to initiate aggregational changes of micelle structure is useful in designing micelle solutions with desired properties for specific applications. The correlation between K_X^{Br} values and the viscoelasticity of the micelle system also supports the use of the semi-empirical kinetic method and Pseudophase Micellar model in other micelle systems.

Declaration of Competing Interest

The author declares that there is no known competing financial interests or personal relationships that could have appeared to influence the work reported in this paper.

Acknowledgement

The work was supported by FSUMRG-KIMIA-17 grant from Universiti Malaya, and FP038-2019A FRGS grant from The Ministry of Higher Education, Malaysia.

References:

[1] M.S. Santos, F.W. Tavares, E.C. Biscaia Jr, Braz. J. Chem. Eng. 33 (2016) 515–523.
[2] R. Pool, P.G. Bolhuis, J. Phys. Chem. B 109 (2005) 6650–6657.
[3] Y. Moroi, R. Matuura, Bull. Chem. Soc. Jpn. 61 (1988) 333–339.
[4] D. Stigter, J. Colloid Interface Sci. 47 (1974) 10.
[5] N.S.M. Yusof, M. Ashokkumar, Soft Matter 9 (2013) 1997–2002.
[6] C.O. Rangel-Yagui, H.W.L. Hsu, A. Pessoa-Jr, L.C. Tavares, Revista Brasileira de Ciências Farmacêuticas 41 (2005) 237–246.
[7] V.P. Torchilin, A.N. Lukyanov, Z. Gao, B. Papahadjopoulos-Sternberg, Proc. Natl. Acad. Sci. 100 (2003) 6039.
[8] P. Ekwall, J. Colloid Interface Sci. 29 (1969) 16–26.
[9] N. Pilpel, Nature 204 (1964) 378–379.
[10] K.S. Lee, J.H. Lee, Chapter 4 - Hybrid Chemical EOR Using Low-Salinity and Smart Waterflood, in: K.S. Lee, J.H. Lee (Eds.) Hybrid Enhanced Oil Recovery using Smart Waterflooding, Gulf Professional Publishing, 2019, pp. 65-110.
[11] M. Atiqullah, A.H. Al-Sarkhi, F.M. Al-Thenayan, A.R. Al-Malki, H.S. Alasiri, Catalysts 9 (2019).
[12] L.Z. Jacques, L. Bin, B. Hans-Werner, Rev. Chem. Eng. 14 (1998) 253–320.
[13] Y. Wang, B. Yu, J.L. Zakin, H. Shi, Adv. Mechan. Eng. 3 (2011), 478749.
[14] A. Kapse, N. Anup, V. Patel, G.K. Saraogi, D.K. Mishra, R.K. Tekade, Chapter 6 - Polymeric micelles: a ray of hope among new drug delivery systems, in: R.K. Tekade (Ed.) Drug Delivery Systems, Academic Press2020, pp. 235-289.
[15] K. Nakamura, T. Shikata, Langmuir 22 (2006) 9853–9859.
[16] Z. Zhai, X. Yan, Z. Song, S. Shang, X. Rao, Soft Matter 14 (2018) 499–507.
[17] R. Messager, A. Ott, D. Chatenay, W. Urbach, D. Langevin, Phys. Rev. Lett. 60 (1988) 1410–1413.
[18] C. Tanford, Proceed. Natl. Acad. Sci. U.S.A 71 (1974) 1811–1815.
[19] A. Shiloach, D. Blankschtein, Langmuir 14 (1998) 7166–7182.
[20] Sunaina, V. Sethi, S.K. Mehta, A.K. Ganguli, S. Vaidya, PCCP 21 (2019) 336–348.
[21] N.S. Yusof, M.N. Khan, Adv Colloid Interface Sci 193–194 (2013) 12–23.
[22] N. Kamaly, Z. Xiao, P.M. Valencia, A.F. Radovic-Moreno, O.C. Farokhzad, Chem. Soc. Rev. 41 (2012) 2971–3010.
[23] G.S. Custer, H. Xu, S. Matysiak, P. Das, Langmuir 34 (2018) 12590–12599.
[24] P. Wang, W. Kang, H. Yang, X. Yin, Y. Zhao, Z. Zhu, X. Zhang, RSC Adv. 7 (2017) 37699–37705.
[25] H. Lu, C. Zheng, M. Xue, Z. Huang, PCCP 18 (2016) 32192–32197.
[26] K. Streletzky, G.D.J. Phillies, Langmuir 11 (1995) 42–47.
[27] B. Hammouda, J. Res. Natl. Inst. Stand. Technol. 118 (2013) 151–167.
[28] W. Yuan, W. Guo, Polym. Chem. 5 (2014) 4259–4267.
[29] J. Wang, M. Pelletier, H. Zhang, H. Xia, Y. Zhao, Langmuir 25 (2009) 13201–13205.
[30] N.S. Yusof, M. Ashokkumar, Ultrason Sonochem 24 (2015) 8–12.
[31] M.N. Khan, J. Chem. Soc. Perkin Trans. 2 (1989) 199–208.
[32] V. Srinivasan, D. Blankschtein, Langmuir 19 (2003) 9932–9945.
[33] C.A. Bunton, L.B. Robinson, J. Organ. Chem. 34 (1969) 773–780.
[34] L.R. Romsted, E.H. Cordes, J. Am. Chem. Soc. 90 (1968) 4404–4409.
[35] E. Iglesias, J.R. Leis, M.E. Pena, Langmuir 10 (1994) 662–669.
[36] C. Bravo, P. Herves, J. Ramon Leis, M. Elena Peña, J. Colloid Interface Sci. 153 (1992) 529–536.
[37] L.J. Magid, Z. Han, G.G. Warr, M.A. Cassidy, P.D. Butler, W.A. Hamilton, J. Phys. Chem. B 101 (1997) 7919–7927.
[38] I.M. Cuccovia, I.N. da Silva, H. Chaimovich, L.S. Romsted, Langmuir 13 (1997) 647–652.
[39] E. Mendes, J. Narayanan, R. Oda, F. Kern, S.J. Candau, C. Manohar, J. Phys. Chem. B 101 (1997) 2256–2258.
[40] P.A. Hassan, B.S. Valaulikar, C. Manohar, F. Kern, L. Bourdieu, S.J. Candau, Langmuir 12 (1996) 4350–4357.
[41] D.A. Mahmood M.E., Al Koofee, Global Journal of Science Frontier Research Chemistry, 13 (2013) 1-7.
[42] M. Niyaz Khan, J. Phys. Org. Chem. 9 (1996) 295–300.
[43] F.M. Menger, C.E. Mounier, J. Am. Chem. Soc. 115 (1993) 12222–12223.
[44] A. Heindl, J. Strnad, H.H. Kohler, J. Phys. Chem. 97 (1993) 742–746.
[45] A. Fernandez, E. Iglesias, L. Garcia-Rio, J.R. Leis, Langmuir 11 (1995) 1917–1924.
[46] N.J. Buurma, Herranz, A. M., & Engberts, J. B. F. N., J. Chem. Soc.-Perkin Trans. 2, 15 (1999) 7.
[47] E.H. Cordes, Pure Appl. Chem. 50 (1978) 9.
[48] N.S.M. Yusof, M.N. Khan, Langmuir 26 (2010) 10627–10635.
[49] R. Germani, G. Savelli, T. Romeo, N. Spreti, G. Cerichelli, C.A. Bunton, Langmuir 9 (1993) 55–60.
[50] A. Blaskó, C.A. Bunton, H.J. Foroudian, J. Colloid Interface Sci. 175 (1995) 122–130.
[51] D.G. Hall, J. Phys. Chem. 91 (1987) 4287–4297.
[52] E. Manousaki, E. Psillakis, N. Kalogerakis, D. Mantzavinos, Water Res. 38 (2004) 3751–3759.
[53] N. Miyoshi, T. Takeshita, V. Misik, P. Riesz, Ultrason. Sonochem. 8 (2001) 367–371.
[54] I.G. Vorobiova, Y.A. Mirgorod, A.S. Chekadanov, J. Nano- and Electron. Phys. 10 (2018) 06013–06017.
[55] J. Moghimi-Rad, T.D. Isfahani, I. Hadi, S. Ghalamdaran, J. Sabbaghzadeh, M. Sharif, Appl. Nanosci. 1 (2011) 27–35.
[56] Sonochemistry, Kirk-Othmer Encyclopedia of Chemical Technology.
[57] S.-H. Cho, J.-Y. Kim, J.-H. Chun, J.-D. Kim, Colloids Surf., A 269 (2005) 28–34.